Journal of Cerebral Blood Flow & Metabolism (2011) 31, 1942–1957

www.jcbfm.com

Connexin channels provide a target to manipulate brain endothelial calcium dynamics and blood–brain barrier permeability

Marijke De Bock[1], Maxime Culot[2], Nan Wang[1], Mélissa Bol[1], Elke Decrock[1], Elke De Vuyst[1], Anaelle da Costa[2], Ine Dauwe[3], Mathieu Vinken[4], Alexander M Simon[5], Vera Rogiers[4], Gaspard De Ley[6], William Howard Evans[7], Geert Bultynck[8], Geneviève Dupont[9], Romeo Cecchelli[2] and Luc Leybaert[1]

[1]*Department of Basic Medical Sciences, Physiology Group, Ghent University, Ghent, Belgium;* [2]*Laboratoire de Physiopathologie de la Barrière Hémato-Encéphalique, Faculté Jean Perrin, Université Lille Nord de France, Lens, France;* [3]*Department of Neurology, Laboratory for Clinical and Experimental Neurophysiology, Ghent University, Ghent, Belgium;* [4]*Department of Toxicology, Vrije Universiteit Brussel, Brussels, Belgium;* [5]*Department of Physiology, College of Medicine, University of Arizona, Tucson, Arizona, USA;* [6]*Department of Anaesthesiology, Ghent University, Ghent, Belgium;* [7]*Department of Medical Biochemistry and Immunology, Cardiff University Medical School, Cardiff, UK;* [8]*Department of Molecular Cell Biology, Laboratory of Molecular and Cellular Signaling, KU Leuven, Leuven, Belgium;* [9]*Theoretical Chronobiology Unit, Université Libre de Bruxelles, Brussels, Belgium*

The cytoplasmic Ca^{2+} concentration ($[Ca^{2+}]_i$) is an important factor determining the functional state of blood–brain barrier (BBB) endothelial cells but little is known on the effect of dynamic $[Ca^{2+}]_i$ changes on BBB function. We applied different agonists that trigger $[Ca^{2+}]_i$ oscillations and determined the involvement of connexin channels and subsequent effects on endothelial permeability in immortalized and primary brain endothelial cells. The inflammatory peptide bradykinin (BK) triggered $[Ca^{2+}]_i$ oscillations and increased endothelial permeability. The latter was prevented by buffering $[Ca^{2+}]_i$ with BAPTA, indicating that $[Ca^{2+}]_i$ oscillations are crucial in the permeability changes. Bradykinin-triggered $[Ca^{2+}]_i$ oscillations were inhibited by interfering with connexin channels, making use of carbenoxolone, Gap27, a peptide blocker of connexin channels, and Cx37/43 knockdown. Gap27 inhibition of the oscillations was rapid (within minutes) and work with connexin hemichannel-permeable dyes indicated hemichannel opening and purinergic signaling in response to stimulation with BK. Moreover, Gap27 inhibited the BK-triggered endothelial permeability increase in *in vitro* and *in vivo* experiments. By contrast, $[Ca^{2+}]_i$ oscillations provoked by exposure to adenosine 5′ triphosphate (ATP) were not affected by carbenoxolone or Gap27 and ATP did not disturb endothelial permeability. We conclude that interfering with endothelial connexin hemichannels is a novel approach to limiting BBB-permeability alterations.
Journal of Cerebral Blood Flow & Metabolism (2011) **31,** 1942–1957; doi:10.1038/jcbfm.2011.86; published online 8 June 2011

Keywords: blood–brain barrier; brain edema; brain ischemia; calcium; endothelium

Introduction

The blood–brain barrier (BBB) is a highly selective lipophilic barrier between the systemic blood circulation and the brain tissue and has an essential role in brain homeostasis, which is crucial for normal neuronal activity and brain function. The BBB is formed by bovine brain capillary endothelial cells (BCECs) that are characterized by an extremely low rate of transcytosis and form a restrictive barrier to paracellular diffusion due to the absence of fenestrations and the presence of a complex structure of tight junctions (Zlokovic, 2008). During neuroinflammation

Correspondence: Professor L Leybaert, Department of Basic Medical Sciences, Physiology Group, Ghent University, De Pintelaan 185, Building B (Rm 310), B-9000 Ghent, Belgium.
E-mail: luc.leybaert@ugent.be
MDB is supported by the Institute for the Promotion of Innovation of Science and Technology in Flanders (IWT Vlaanderen—Grant number 63352). LL is granted by the Fund for Scientific Research Flanders (FWO—Grant numbers G.0140.08 and 3G.0134.09, G.0298.11N and WO.005.10N) and the Interuniversity Attraction Poles Program (Belgian Science Policy Project P6/31). GD is 'Maître de Recherche' at the Belgian 'Fonds de la Recherche Scientifique' (FNRS). AMS is granted by the NIH (HL64232).
Received 29 December 2010; revised 8 April 2011; accepted 10 May 2011; published online 8 June 2011

and stroke, BBB endothelial cells loose their barrier properties, leading to uncontrolled passage of ions, proteins, and water that culminates in disturbed neural tissue functioning and edema. The detailed signal-transduction pathways leading to BBB alterations, including increased permeability of the endothelial layer, are complex and not fully understood, but it is well appreciated that an increase in the cytosolic Ca^{2+} concentration ($[Ca^{2+}]_i$ takes a central stage in this process (Abbott, 2000). Bradykinin (BK), a nonapeptide derived from the kinin-kallikrein system, is a typical inflammatory messenger that triggers a BBB permeability increase both *in vitro* (Easton and Abbott, 2002; Hurst and Clark, 1998) and *in vivo* (Sarker *et al*, 2000). Genetic knockout of the G-protein coupled BK receptor-1 or pharmacological interference with this receptor protects mice against BBB permeability increases and brain edema following stroke (Austinat *et al*, 2009) and brain trauma (Raslan *et al*, 2010). $[Ca^{2+}]_i$ was identified as the major second messenger mediating the downstream effects of BK (Easton and Abbott, 2002; Olesen, 1989). RMP7, a stable analog of BK used clinically to increase barrier permeability to drugs, mimics BK in its capability to increase $[Ca^{2+}]_i$ (Doctrow *et al*, 1994). Investigations on BK-triggered $[Ca^{2+}]_i$ changes have been limited to studies that focus on the initial $[Ca^{2+}]_i$ transient provoked by exposing endothelial cells to BK. However, it is unlikely that a single short-lived $[Ca^{2+}]_i$ elevation would be sufficient to induce longer-lived BBB alterations. Ongoing repetitive $[Ca^{2+}]_i$ spike activity, that is $[Ca^{2+}]_i$ oscillations, are more likely to result in prolonged alterations in BBB function. $[Ca^{2+}]_i$ oscillations have been demonstrated in BBB endothelial cells, in response to adenosine 5′ triphosphate (ATP) (Haorah *et al*, 2007), hypoxia (Brown *et al*, 2004), endothelial–leukocyte interactions (Etienne-Manneville *et al*, 2000), or invasion of bacteria (Nikolskaia *et al*, 2006) but little is known on their effect on BBB function. BK has been demonstrated to trigger $[Ca^{2+}]_i$ oscillations in endothelia from various vascular beds and species (Carter *et al*, 1991; Laskey *et al*, 1992; Sage *et al*, 1989) but it is not known whether this is also the case in BBB endothelium.

A starting point for the present study was the observation by Kawano *et al* (2006), that in human mesenchymal stem cells, $[Ca^{2+}]_i$ oscillations are linked to connexin hemichannels, which are unapposed hexameric plasma membrane channels not engaged into gap junctions. The linkage factor was that ATP, released via hemichannels, activates $P2Y_1$ receptors and subsequently stimulates phospholipase C (PLC)-β with activation of $InsP_3$ signaling that lies at the basis of $[Ca^{2+}]_i$ oscillations (Dupont *et al*, 2007). A second link, provided by Verma *et al* (2009), demonstrated inhibition of $[Ca^{2+}]_i$ oscillations in cardiomyocytes and other cells by connexin mimetic peptides, which are synthetic peptides composed of a short sequence of the connexin protein, the building block of hemichannels and gap junctions. Finally, Nagasawa *et al* (2006) provided evidence, in a porcine BBB model, that endothelial connexins are associated with tight junction proteins and that inhibition of gap junctions inhibited barrier function. The aim of the present work was to investigate the role of connexin channels in endothelial $[Ca^{2+}]_i$ oscillations and BBB function, and to determine whether these channels can be used as a target to prevent BBB alterations. We used ATP and BK as inducers of $[Ca^{2+}]_i$ oscillations and assessed their effect on endothelial permeability as a parameter of BBB function. Interestingly, we found that interfering with connexin channels by using carbenoxolone, siRNA silencing of endothelial connexins (Cx37 and Cx43), and Gap27, a peptide identical to a sequence on the second extracellular loop of Cx37 and Cx43, inhibited $[Ca^{2+}]_i$ oscillations triggered by BK but not those triggered by ATP. Endothelial permeability measurements *in vitro* demonstrated that the BK-triggered permeability increase was inhibited by Gap27 and this was further confirmed by *in vivo* BBB permeability measurements. Collectively, these data suggest that the connexin channel linkage of BK-triggered $[Ca^{2+}]_i$ oscillations, which is absent in ATP-triggered oscillations, has a role in influencing BBB permeability. Further work with connexin channel-permeable dyes indicated that BK exposure induced the opening of connexin hemichannels and that Gap27 inhibition of the oscillations was related to inhibition of hemichannels. These results demonstrate that connexin channel-linked $[Ca^{2+}]_i$ oscillations are involved in controlling BBB permeability and that interfering with endothelial connexins is a novel approach to limit BBB permeability increases.

Materials and methods

Cell Culture

RBE4 (rat brain endothelial) cells were kindly provided by Dr Françoise Roux (Neurotech, Evry, France). Cells (up to passage 25) were grown on collagen-coated recipients (rat-tail collagen; Roche Diagnostics, Vilvoorde, Belgium) and maintained in α-minimal essential medium (MEM)/Ham's F10 (1:1) supplemented with 10% fetal calf serum, 2 mmol/L glutamine, 300 μg/mL G-418 (Gibco, Invitrogen, Merelbeke, Belgium), and 1 ng/mL human recombinant basic fibroblast growth factor (Roche Diagnostics) at 37°C and 5% CO_2. Bovine BCECs were grown in a noncontact coculture with rat mixed glial cells as described previously (Cecchelli *et al*, 1999). Glial cells were isolated from Sprague Dawley rat cerebral cortex at postnatal day 3, according to the procedure described by Descamps *et al* (2003). Briefly, meninges were removed and brain tissue was gently forced through a nylon sieve. Glial cell cultures were obtained by seeding the cells on six-well plates at 10^5 cells in Dulbecco's modified Eagle medium (DMEM) supplemented with 10% fetal calf serum. Immunostainings showed that these cultures contained ~76% glial fibrillary acidic protein (GFAP)-positive cells (astrocytes), ~18% ectodermal dysplasia-1 (ED-1)-positive cells (microglia), and ~6% O4-positive

cells (oligodendrocytes). Three weeks after seeding, glial cultures were ready for use in coculture experiments. Bovine brain capillary endothelial cells, seeded onto rat-tail collagen-coated polycarbonate filter inserts (Millicell-PC, 3 μm pore size, 30 mm diameter, Millipore Corporation, Molsheim, France) were placed into six-well plates containing the glial cells. BCEC and glia were grown together for another 12 days after which BBB features fully developed. During this period, cells were kept in DMEM supplemented with 10% newborn calf serum, 10% horse serum, 2 mmol/L L-glutamine, 50 μg/mL gentamycin, and 1 ng/mL basic fibroblast growth factor. HeLa cells (kindly provided by Dr Klaus Willecke, Universität Bonn, Germany) and C6-glioma cells (kind gift of Dr Christian C Naus, University of British Columbia, Canada) were maintained in DMEM and DMEM/Ham's F12 (1:1), respectively, supplemented with 10% fetal calf serum and 2 mmol/L glutamine.

Chemicals and Reagents

Adenosine 5′ triphosphate (ATP), 2-(methylthio)-ATP (2-MeS-ATP), ARL-67156, apyrase grade VI and VII, BK, carbenoxolone, ethylene glycol-bis-(β-aminoethyl ether)-*N,N,N′,N′*-tetraacetic acid (EGTA), paraformaldehyde, PPADS (pyridoxal phosphate-6-azo(benzene-2,4-disulfonic acid) tetrasodium salt), probenecid, and suramin were purchased from Sigma-Aldrich (Bornem, Belgium). 1,2-bis-(2-aminophenoxy)-ethane-*N,N,N′,N′*-tetraacetic acid acetoxy methyl ester (BAPTA-AM), calcein-AM, 5-CFDA-AM (5-carboxyfluorescein diacetate acetoxy methyl ester), 3 kDa dextran fluorescein (DF) (lysine-fixable), 10 kDa dextran texas red, fluo3-AM, Hoechst 33342, lucifer yellow (LY), pluronic acid F-127 and propidium iodide (PI) were from Molecular probes (Invitrogen, Merelbeke, Belgium). D-*myo*-inositol 1,4,5-trisphosphate, $P^{4(5)}$-1-(2-nitrophenyl)ethylester ('caged-$InsP_3$') was from Calbiochem. The Gap27 peptide (SRPTEKTIFII—position 201 to 210 in both Cx37 and Cx43) and scrambled Gap27 ($Gap27^{Scr}$, TFEPIRISITK) were synthesized by Thermo Fisher Scientific (Ulm, Germany) at >80% purity.

$[Ca^{2+}]_i$ Imaging

RBE4 cells were seeded onto 9.2 cm^2 petridishes (TPP, Novolab, Geraardsbergen, Belgium) and experiments were performed at confluency. RBE4 monolayers were loaded with a mixture of 10 μmol/L fluo3-AM, 1 mmol/L probenecid, and 0.01% pluronic acid in HBSS-Hepes (in mmol/L: 0.95 $CaCl_2$; 0.81 $MgSO_4$; 13 NaCl; 0.18 Na_2HPO_4; 5.36 KCl; 0.44 KH_2PO_4; 5.55 D-glucose; and 25 Hepes) during 1 hour at room temperature (RT). BCECs on filter inserts were placed in petridishes with HBSS-Hepes/probenecid containing fluo3-AM (10 μmol/L) and pluronic acid (0.01%). The same solution was added to the filter insert. After 1 hour, petridishes (RBE4) or filter inserts (BCECs) were washed and cells were left for an additional 30 minutes at RT in HBSS-Hepes/probenecid to allow for deesterification. Cells were thereafter transferred to an inverted epifluorescence microscope (Eclipse TE 300, Nikon Belux, Brussels, Belgium), equipped with a heating stage to maintain the cells at ~27°C. A superfusion system allowed changing the bath solution within ~1 minute (bath volume ~1 mL). Superfusion was switched off during the registration of oscillatory activity. Images were taken every second with a ×40 water immersion objective (NA 0.8) and an electron multiplying CCD camera (Quantem 512SC; Photometrics, Tucson, AZ, USA). We used a Lambda DG-4 filterswitch (Sutter Instrument Company, Novato, CA, USA) to deliver excitation at 482 nm and captured emitted light via a 505-nm long-pass dichroic mirror and a 535-nm bandpass filter (35 nm bandwidth). Recordings and analysis were performed with custom-developed QuantEMframes and Fluoframes software written in Microsoft Visual C^{++} 6.0. Ca^{2+} oscillations were counted in a 10-minute observation period and were defined as at least two transient Ca^{2+} changes subsequent to the initial Ca^{2+} transient in a single cell, minimally 10% above baseline fluo3-fluorescence.

Caged-$InsP_3$ Loading and Photoliberation

C6-glioma cells were loaded with caged-$InsP_3$ by electroporation, as described before (Decrock *et al*, 2009). Briefly, cells, grown to confluency, were rinsed with a low-conductivity electroporation buffer and placed on the microscope stage. Thereafter, a small volume (10 μL) of caged-$InsP_3$ (200 μmol/L) and 10 kDa dextran texas red (100 μmol/L, added to visualize the electroporation zone), dissolved in electroporation buffer was added to a parallel wire Pt-Ir-electrode, positioned 400 μm above the cells. Electroporation was performed with 50 kHz bipolar pulses, at a field strength of 1,000 V/cm, applied as 15 trains of 10 pulses of 2 milliseconds duration each. After electroporation, cells were washed with HBSS-Hepes, left 5 minutes to recover and finally loaded with fluo3-AM. Photoliberation of $InsP_3$ was performed by spot (20 μm diameter) illumination with 1 kHz pulsed ultraviolet light (349 nm ultraviolet laser Explorer, Spectra-Physics, Newport, Utrecht, The Netherlands) applied during 20 milliseconds (20 pulses of 90 μJ energy measured at the entrance of the microscope epifluorescence tube).

Gap Junction Dye Coupling Studies

Dye coupling via gap junctions was determined making use of fluorescence recovery after photobleaching. Endothelial cultures were grown confluent on 9.2 cm^2 petridishes (TPP) and were loaded with the gap junction permeable fluorescent dye 5-CFDA-AM (532 Da, 10 μmol/L) in HBSS-Hepes/probenecid for 1 hour at RT. Following deesterification, cells were transferred to a custom-made video-rate confocal laser scanning microscope with a ×40 water immersion objective (CFI Plan Fluor, Nikon Belux, Brussels, Belgium) and a 488-nm laser excitation source (Cyan CW Laser, 488 nm to 100 mW, Newport Spectra-Physics). After 1 minute of recording, the cell in the middle of the field was photobleached by spot exposure (1 second) to increased power of the 488-nm laser and fluorescence recovery, caused by dye influx from neighboring nonbleached cells, was recorded during an additional 5-minute period. The fluorescence recovery trace was then analyzed for the recovery of the signal expressed relative to the starting level before photobleaching.

Hemichannel Assays

Hemichannel opening was investigated by the uptake or release of fluorescent hemichannel-permeable dyes. We used calcein (623 Da) to study dye release and PI (668 Da), LY (457 Da), or 3 kDa DF to investigate dye uptake. The latter was used as a hemichannel-impermeable control probe (Li *et al*, 1996). Calcein release is based on the efflux of the preloaded dye via hemichannels. For calcein release studies, subconfluent cultures of RBE4, grown on glass coverslips, were preloaded with 50 μmol/L calcein-AM in HBSS-Hepes/probenecid for 1 hour at RT. Subsequently, the remaining calcein-AM was removed; cells were left to deesterify an additional 30 minutes at RT in HBSS-Hepes/probenecid and were then transferred to an inverted epifluorescence microscope. For analysis, we measured the decrease in calcein fluorescence as a function of time. The first 5 minutes baseline leakage in HBSS-Hepes/probenicid (control) was measured. Thereafter, the trigger solution was added and efflux of calcein was further evaluated during 5 minutes. Gap27 was either preincubated during 1 hour or added together with the trigger for an additional 5 minutes in superfusion experiments. The slope of the curve, calculated by linear regression, was used as a parameter describing the loss of dye in time. Calcein efflux in the presence of trigger is presented as percentage of control. For dye uptake, cells were seeded onto four-well plates (Nunc brand products, Novolab) at a density of 50,000 cells/mL and used the next day. Cultures were rinsed twice and incubated during 10 minutes with PI (2 mmol/L), LY (25 mmol/L), or 3 kDa DF (100 μmol/L) added to the trigger solution. Pictures were acquired with a Nikon TE 300 epifluorescence microscope, $\times 10$ objective (Plan APO, NA 0.45) and Nikon DS-5M camera (Nikon Belux). In each culture, nine snap-shot images were taken. The number of dye-positive cells in each image was counted using ImageJ (NIH, Bethesda, MD, USA; http://rsb.info.nih.gov/ij) after application of a threshold corresponding to the upper level of the background signal. Dye uptake is expressed as the percentage of dye-positive cells relative to the total number of cells counted with Hoechst staining ($22{,}000 \pm 900$ cells/cm^2).

Cell Death Studies

Cell death was assessed by examining PI uptake into the cells. Cell cultures were exposed to PI (30 μmol/L) and Hoechst (10 μg/mL) for 10 minutes. The number of death cells showing PI staining was expressed as the percentage of dye-positive cells relative to the total number of cells counted from the Hoechst staining. Note that PI was also used for dye uptake studies, which needed much higher concentrations (see 'Hemichannel assays').

In Vitro Endothelial Permeability

In vitro endothelial permeability was measured as described previously (Cecchelli *et al*, 1999). Filter inserts containing confluent BCEC monolayers were separated from the glial cells, washed with HBSS-Hepes, and added to a six-well plate with each well containing 2.5 mL HBSS-Hepes (lower compartment). The filter insert (upper compartment) was filled with 1.5 mL HBSS-Hepes containing 50 μmol/L LY (457 Da) or 3 kDa DF (20 μmol/L) as a transport marker. At 15, 30, 45, and 60 minutes, the filters were transferred to a new well (Figure 5A) and samples were taken from each lower compartment. The temperature was kept at 37°C. Aliquots were also taken from the upper compartment, at the beginning and end of the experiment. The cleared volume was determined by dividing the fluorescence in the lower compartment at each time point by the concentration in the upper compartment and was plotted versus time. The slope of this curve, calculated by linear regression, corresponds to the permeability-surface (PS) product and subtracting the PS product of an empty, coated filter gives the PS product of the endothelial monolayer. Subsequent division by the surface area of the filter membrane (4.2 cm^2) yields the permeability coefficient Pe. The inhibitory agents and vehicles used in this study were all without effect on the permeability.

In Vivo Blood–Brain Barrier Permeability

Male Wistar rats (200 to 250 g) were treated according to the European Ethics Committee guidelines and the study protocol was approved by the university animal experiment ethical committee. The animals were housed under controlled environmental conditions with *ad libitum* access to food and water and were randomly assigned to treatment ('control,' 'BK', 'BK + Gap27', or 'BK + Gap27^{Scr}'). On the same day, rats were anesthetized with sodium pentobarbital (100 mg/kg, intraperitoneally) and a catheter (PE 50) was placed in the femoral vein. Control rats received 3 kDa DF (30 mg/kg, intravenously), 'BK rats' received 3 kDa DF in combination with BK (150 μg/kg, intravenously) and in 'BK + Gap27' or 'BK + Gap27^{Scr}' rats 3 kDa DF was administered along with BK (150 μg/kg, intravenously) and Gap27 or Gap27^{Scr}, respectively, (both 25 mg/kg, intravenously). All solutions were allowed to circulate during 30 minutes. Subsequently, the animals were transcardially perfused, first with PBS and in second instance with 4% paraformaldehyde to fix the tissue. Immediately after isolation, the brain was sliced into thick (± 2 mm) coronal sections using a vibrating microtome (Vibroslice 725 mol/L; Campden Instruments Ltd., Loughborough, UK). The area from which sections were made was located between 4.7 mm anterior and 7.3 mm posterior to the bregma. Brain sections were visualized using a GeneFlash system (Syngene, Cambridge, UK) equipped with a ultraviolet light source, a 410 to 510 nm conversion screen, CCD camera, f/1.2 8 to 48 mm zoom lens and an emission bandpass filter to detect fluorescence (550 to 600 nm). The signal intensity was determined using ImageJ software. For each section, fluorescence intensity was determined in 10 zones, all located in the cortex that was identified by comparison of visible light images with a rat brain atlas. Background fluorescence was measured just outside the coronal sections and was subtracted from the fluorescence in the measurements points.

siRNA Treatment

RBE4 cells were seeded on 9.2 cm^2 dishes at 27,000 cells/cm^2 and transfected the following day with 50 nmol/L siGENOME ON-TARGETplus SMARTpool siRNA using Dharmafect1 lipid reagent (Dharmacon, Thermo Fisher Scientific, Erembodegem, Belgium). The siRNA pool used was a mix of four different duplexes directed against the Cx37 gene gja4 and the Cx43 gene gja1 (rat). On day 3, culture medium was refreshed and on day 4, cells were used for experiments. Transfection efficiency was 51% ± 2.0% ($n = 16$) on day 3, as determined with the fluorescent indicator siGLO. Control conditions were untreated cultures, Mock-treated cultures (lipid reagent alone), and a negative control consisting of cultures transfected with a pool of four duplexes that have minimal targeting of known rat genes (ON-TARGETplus siCONTROL nontargeting pool—Dharmacon). Western blotting demonstrated that siRNA pools targeting Cx37 and Cx43 reduced the expression of their respective target in RBE4 cells, but there were crossreactions from the Cx43 siRNA on Cx37 expression and *vice versa* (caused either by coordinated regulation of Cx37 and Cx43 expression or true crossactivation of the applied siRNAs). We therefore combined the two siRNA treatments to knockdown both Cx37 and Cx43. siRNA treatment of BCECs was not possible as the procedure by itself caused increased permeability of the endothelial cell layer.

Electrophoresis and Western Blotting

For Western blots, cells were seeded in 75 cm^2 falcons or 9.2 cm^2 dishes (siRNA-treated cells). Total RBE4 lysates were extracted with RIPA buffer, BCEC filters were scraped in ice-cold PBS containing protease inhibitor cocktail (Roche Diagnostics). Protein concentration was determined using the Bio-Rad DC protein assay kit (Bio-Rad, Nazareth, Belgium) and absorbance was measured with a 590-nm long-pass filter. The lysate was separated by electrophoresis over a 10% sodium dodecyl sulfate-polyacrylamide gel and transferred to a nitrocellulose membrane (Amersham, Buckinghamshire, UK). Membranes were subsequently blocked with Tris-buffered saline (TBS) containing 5% nonfat milk and 0.1% Tween20. Following the blocking, blots were probed with rabbit anti-Cx43 antibody (Sigma-Aldrich), rabbit anti-Cx40 antibody (α-Diagnostic International, Brussels, Belgium), rabbit anti-Cx37 antibody (gift of AM Simon; (Simon *et al*, 2006)), rabbit anti-$P2X_7$ antibody (Alomone Labs, Jerusalem, Israel), and rabbit anti-β-tubulin antibody (Abcam, Cambridge, UK) as a loading control. Membranes were subsequently incubated with an alkaline phosphatase-conjugated goat anti-rabbit IgG antibody (Sigma-Aldrich) and detection was performed using the nitro-blue-tetrazolium/5-bromo-4-chloro-3-indolyl-phosphate reagent (NBT/BCIP kit, Zymed, Invitrogen, Merelbeke, Belgium). Quantification was performed by drawing a rectangular window around the concerned connexin band and determining the signal intensity using ImageJ. Background correction was performed by the same procedure applied to nitrocellulose membranes where protein was absent.

Polymerase Chain Reaction

Cells were grown to confluence on 75 cm^2 falcons, scraped in ice-cold PBS, and the resulting pellet was put at −80°C. Total RNA was isolated using the RNeasy Plus mini kit (Qiagen, Venlo, The Netherlands). Reverse transcription was performed by the iScript cDNA synthesis kit (Bio-Rad) and cDNA was amplified using the Taq DNA polymerase kit (Invitrogen). Primers were Panx1 forward 5′-TTCT TCCCCTACATCCTGCT-3′ and reverse 5′-GGTCCATCTCT CAGGTCCAA-3′; glyceraldehyde-3-phosphate dehydrogenase (internal control) forward 5′-ACCACAGTCCATG CCATCAC-3′ and reverse 5′-TCCACCACCCTGTTGCT GTA-3′ (all synthesized by Invitrogen). The polymerase chain reaction protocol contained 35 cycles of 94°C (45 seconds), 50°C (1 minute), and 72°C (1 minute), preceded by 4 minutes 94°C and followed by 5 minutes 72°C. As a negative control, a sample lacking reverse transcriptase (RT−) was used. The polymerase chain reaction end products were separated on a 2% agarose gel and visualized with ethidium bromide (Invitrogen).

Immunofluorescence

Immunostaining of BCECs was performed with the following primary antibodies: rabbit anti-occludin, mouse-anti-vimentin and rabbit anti-ZO-1 (all from Zymed Laboratories Inc., Invitrogen). Rhodamine phalloidine (Molecular Probes, Invitrogen) was used for F-actin labeling. Following fixation with 4% paraformaldehyde, cells were permeabilized with 0.1% Triton X-100 or ice-cold acetone (vimentin staining). Cells were then preincubated for 30 minutes in 10% goat serum before addition of primary antibodies (diluted in 2% normal goat serum). After washing, secondary antibody conjugated to Alexa-568 or Alexa-488 (Molecular Probes, Invitrogen) was added and filter sections were mounted in Mowiol containing 1,4-diazabicyclo[2,2,2]octane (DABCO) (Sigma-Aldrich).

Statistical Analysis

Data are expressed as mean ± s.e.m. with n giving the number of independent experiments. Multiple groups were compared by one-way analysis of variance and a Bonferroni posttest, making use of Graphpad Instat software (La Jolla, CA, USA). Two groups were compared with an unpaired Student's t-test and two-tail P value. Results were considered statistically significant when $P < 0.05$ (one symbol for $P < 0.05$, two for $P < 0.01$, and three for $P < 0.001$).

Results

Bradykinin Triggers $[Ca^{2+}]_i$ Oscillations that Involve Connexin Hemichannel Opening and Purinergic Signaling

Exposure of confluent RBE4 cell cultures to BK in the range of 50 nmol/L to 1 μmol/L typically elicited a transient $[Ca^{2+}]_i$ increase, followed by repetitive $[Ca^{2+}]_i$ spikes or oscillations. Occasionally, the initial

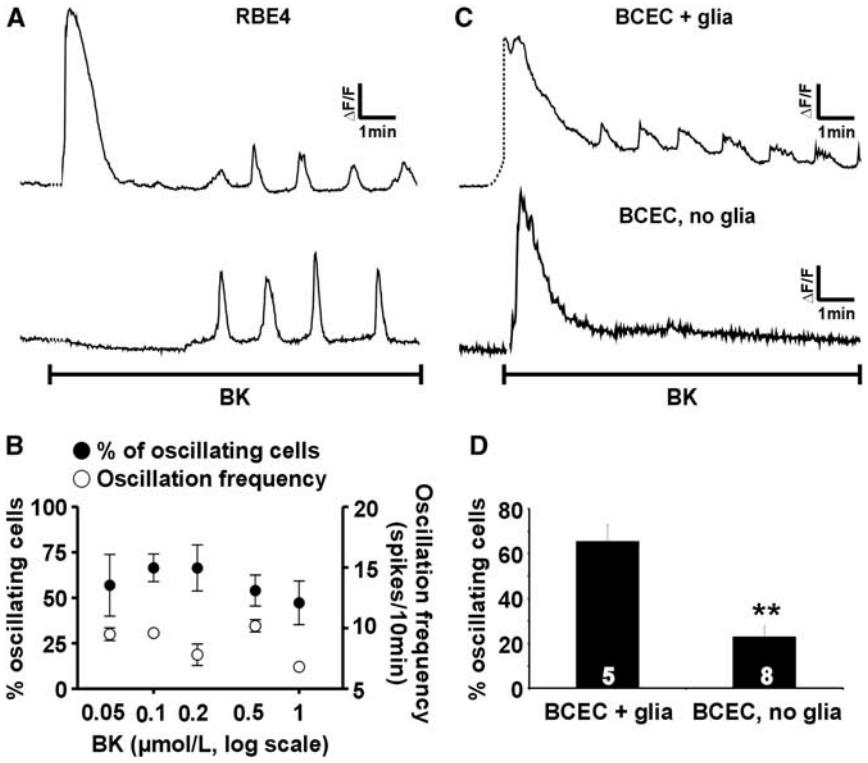

Figure 1 Bradykinin (BK) elicits oscillations in the cytoplasmic Ca^{2+} concentration ($[Ca^{2+}]_i$). (**A**) Example traces of $[Ca^{2+}]_i$ oscillations in selected rat brain endothelial (RBE4) cells (from two different confluent cultures) triggered by 0.5 μmol/L BK. (**B**) The percentage of oscillating cells (●, left ordinate) and the oscillation frequency (○, right ordinate) for various BK concentrations. (**C**) Example traces of $[Ca^{2+}]_i$ oscillations triggered by 0.5 μmol/L BK in bovine brain capillary endothelial cells (BCECs) on membrane inserts grown in the presence (+ glia) or absence (no glia) of mixed glial cells in the bottom dish. (**D**) Summary data of the percentage of oscillating cells in BCECs grown with or without glia, stimulated with 0.5 μmol/L BK.

$[Ca^{2+}]_i$ transient was absent (Figure 1A). Figure 1B depicts the number of oscillating cells and the oscillation frequency, which did not change markedly with the BK concentration. At 0.5 μmol/L (the concentration used in subsequent experiments), the frequency averaged 10 ± 0.5 $[Ca^{2+}]_i$ transients per 10 minutes ($n = 5$), comparable to the BK-triggered oscillation frequency in other cell types (De Blasio *et al*, 2004). There was no apparent synchronization of oscillatory activity between neighboring, oscillating cells. Baseline measurements in vehicle-treated RBE4 cultures showed that $1.8\% \pm 0.9\%$ of the cells were spontaneously oscillating at an average frequency of 2.3 ± 0.2 spikes per 10 minutes ($n = 6$; percentage of oscillating cells significantly lower than following BK stimulation for all concentrations applied; $P < 0.01$). BK exposure of primary bovine BCECs kept in coculture with glial cells (see Materials and methods) gave a similar $[Ca^{2+}]_i$ response pattern as in RBE4, with an initial transient followed by oscillatory activity. Here, baseline conditions showed $5.3\% \pm 1.8\%$ of the cells spontaneously oscillating ($n = 3$; significantly lower than after BK stimulation for all concentrations applied; $P < 0.05$). Interestingly, oscillations in response to 0.5 μmol/L BK were significantly less frequent when BCECs were cultured on membrane inserts without mixed glial cells in the bottom dish (~25% of the cells oscillating versus ~65% with glial cells present during coculture; Figures 1C and 1D).

Previous work in various cell types has suggested that $[Ca^{2+}]_i$ oscillations can be suppressed by interfering with connexin hemichannels (Kawano *et al*, 2006; Verma *et al*, 2009). We tested the effect of two types of blockers: carbenoxolone, a general connexin channel blocker (Giaume and Theis, 2010), and connexin mimetic peptides (Evans *et al*, 2006). The action of the mimetic peptides may depend on the connexin isoforms being present (Evans *et al*, 2006) and we first checked connexin expression in the cells used. Western blot analysis showed Cx37 and Cx43 expression in RBE4 and BCECs (Figure 2A), with no discernable Cx40 signal. The Cx40 signal was also absent in reverse transcriptase polymerase chain reaction experiments on the two cell types (data not shown). Connexin expression was not different between the 'BCEC + glia' and 'BCEC, no glia' conditions, indicating that the strong reduction of $[Ca^{2+}]_i$ oscillations in 'BCEC, no glia' is not caused by changes in connexin expression.

Gap27 is a peptide identical to a short sequence in the second extracellular loop of both Cx37 and Cx43; this peptide has been demonstrated to inhibit connexin hemichannel-mediated ATP release and dye uptake upon short (minutes) exposure (Braet *et al*, 2003; Eltzschig *et al*, 2006; Evans *et al*, 2006),

while longer exposures (several hours) also affect gap junctions (Braet *et al*, 2003; Decrock *et al*, 2009). Figures 2B and 2C demonstrate that 1 hour exposure to Gap27 (200 μmol/L) did not impair gap junctional dye coupling in RBE4 and BCEC cultures measured with fluorescence recovery after photobleaching, while 24 hours incubations indeed inhibited junctional coupling. Gap27 (200 μmol/L, 1 hour preincuba-

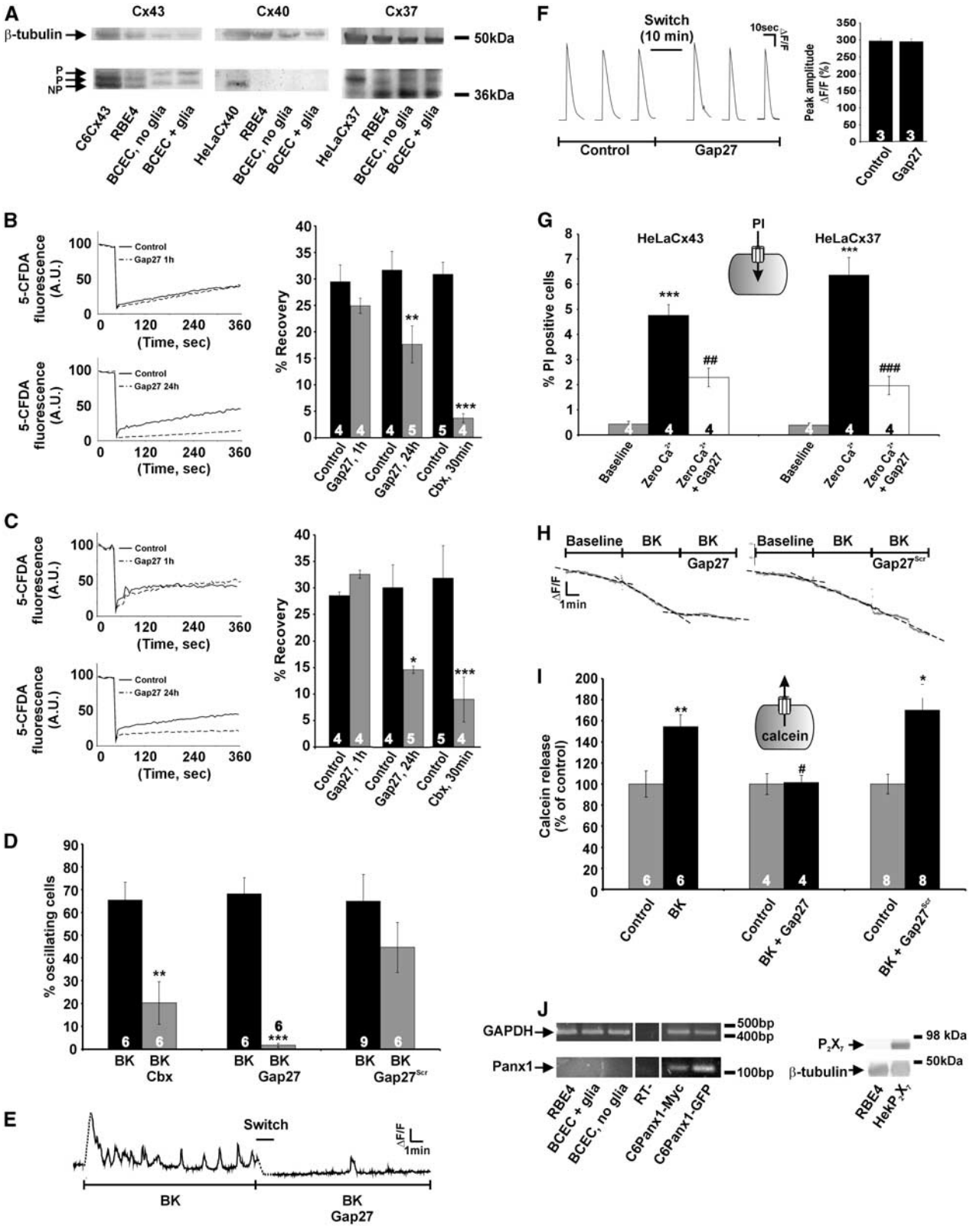

tion) and the nonspecific connexin channel inhibitor carbenoxolone (Cbx, 25 μmol/L, 30 minutes) strongly reduced the number of cells displaying $[Ca^{2+}]_i$ oscillations in response to BK exposure, whereas scrambled Gap27 ($Gap27^{Scr}$) had no effect (Figure 2D). The Gap27 effect on oscillations in individual cells occurred rapidly, within minutes after introducing the peptide in the bath solution (Figure 2E).

$[Ca^{2+}]_i$ oscillations are driven by the concerted action of $InsP_3$ and Ca^{2+} on $InsP_3$ receptors (Dupont *et al*, 2007) and we tested whether Gap27 influenced this signaling pathway. We performed these experiments in C6-glioma cells that have a low endogenous connexin expression to avoid interference of Gap27 with connexin channels. Step-like increases of intracellular $InsP_3$ in these cells, brought about by photoliberation of $InsP_3$, triggered transient $[Ca^{2+}]_i$ changes that were not influenced by Gap27 (Figure 2F). As a consequence, in RBE4, inhibition of oscillations by Gap27 was not caused by influencing $InsP_3$-triggered Ca^{2+} release and we further explored the involvement of connexin hemichannels in BK-triggered oscillations. We used the hemichannel-permeable dye PI (668 Da, charge +2) in dye uptake studies and calcein (623 Da, charge −4, preloaded into the cells) in dye release experiments to document hemichannel opening. Experiments on Cx37- or Cx43-expressing HeLa cells indicated that Gap27 inhibited dye uptake in both cell lines with similar potency (Figure 2G), as expected from the sequence homology of the Gap27 domain in Cx37 and 43. Exposure of RBE4 cells to BK (0.5 μmol/L, 10 minutes) triggered PI uptake (data not shown) and calcein release that was inhibited by Gap27 but not affected by $Gap27^{Scr}$ (Figures 2H and 2I). A contribution of Panx1 hemichannels or $P2X_7$ receptor channels as alternative pathways for dye uptake was excluded based on the absence of mRNA and protein expression, respectively (Figure 2J).

We next applied siRNA technology to silence the two connexin isoforms (Cx37/Cx43) and verified the effect on $[Ca^{2+}]_i$ oscillations. Treatment of RBE4 cells with siRNA directed against Cx37/Cx43 reduced the expression of both connexins by $\sim$1/3 (Figure 3A) and approximately halved the number of oscillating cells during BK exposure (Figure 3B). siRNA treatment did not influence cell death (0.2% ± 0.1% PI-positive cells versus 0.3% ± 0.1% in untreated cells, $n = 6$).

Connexin hemichannel opening results in ATP release (Kang *et al*, 2008) and we tested whether extracellular ATP played a role in the oscillations. The number of RBE4 cells displaying BK-triggered $[Ca^{2+}]_i$ oscillations was strongly reduced by apyrase VI/VII (5 U/mL, 30 minutes preincubation), an enzyme mix that hydrolyzes ATP to AMP, or the two broad spectrum P2 receptor antagonists suramin (200 μmol/L, 30 minutes preincubation) and PPADS (75 μmol/L, 30 minutes preincubation) (Figure 3C). Interestingly, when RBE4 cells were exposed to BK and ATP together (both 0.5 μmol/L), the oscillations disappeared (Figure 3C). We tested lower concentrations of ATP (0.1 and 0.05 μmol/L) coapplied with 0.5 μmol/L BK and this gave an equally strong (and equally significant) inhibition as 0.5 μmol/L. In addition, hemichannel PI uptake studies demonstrated less PI-positive cells when ATP was coadministered with BK (both at 0.5 μmol/L) as compared with BK alone (Figure 3D).

Adenosine 5′ Triphosphate Triggers $[Ca^{2+}]_i$ Oscillations that Are not Associated with Hemichannel Opening

Exposing RBE4 or BCECs (cocultured with glial cells) to ATP (25 nmol/L to 1 μmol/L) triggered $[Ca^{2+}]_i$ oscillations (Figure 4A) and the oscillation frequency increased with ATP concentration (from 6 to 11 Ca^{2+}

Figure 2 Connexin channels are involved in bradykinin (BK)-triggered oscillations in the cytoplasmic Ca^{2+} concentration ($[Ca^{2+}]_i$). (**A**) Western blot analysis for Cx37, Cx40, and Cx43 in rat brain endothelial (RBE4) cells and bovine brain capillary endothelial cells (BCECs). Cx43 and Cx37 were present whereas Cx40 was not detected. C6Cx43, HeLaCx40, and HeLaCx37 were positive controls; β-tubulin was a loading control. (**B**) Gap junctional dye coupling studied with fluorescence recovery after photobleaching in RBE4 cultures. Gap27 (200 μmol/L) did not influence dye coupling (quantified from fluorescence recovery) after 1 hour incubation but inhibited coupling following 24 hours incubation. The general connexin channel blocker carbenoxolone (Cbx, 25 μmol/L) was used as a positive control. Star signs compare to control. (**C**) Similar observations were made in BCECs. (**D**) In RBE4 cells, $[Ca^{2+}]_i$ oscillations elicited by 0.5 μmol/L BK were inhibited by Cbx (25 μmol/L, 30 minutes) and Gap27 (200 μmol/L, 1 hour) but not by $Gap27^{Scr}$ (200 μmol/L, 1 hour). Stars compare to BK. (**E**) Example trace illustrating rapid block of BK-induced $[Ca^{2+}]_i$ oscillations after adding Gap27 ('switch,' 1 minute duration). (**F**) Gap27 does not disturb $InsP_3$-Ca^{2+} signaling. Example traces of $[Ca^{2+}]_i$ transients triggered by photoactivation of $InsP_3$ in C6-glioma cells under control conditions and in the presence of Gap27 (200 μmol/L, 10 minutes). The bar chart at the right summarizes the results of these experiments: Gap27 had no influence on the peak amplitude of $InsP_3$-induced $[Ca^{2+}]_i$ changes. (**G**) Experiment demonstrating that Gap27 inhibited propidium iodide (PI) uptake in HeLa cells expressing Cx37 (HeLaCx37) and in HeLaCx43. Hemichannel opening was stimulated by exposure of the cells to zero extracellular Ca^{2+} solution and the percentage of PI-positive cells was determined. Stars compare to baseline; number signs compare to zero Ca^{2+}. (**H**) Exposure of RBE4 cells preloaded with calcein (ester loading) to BK (0.5 μmol/L) stimulated the loss of calcein from the cells and this was rapidly inhibited by Gap27 (200 μmol/L) but not by $Gap27^{Scr}$. The dashed lines represent linear fits of the three trace sections. (**I**) Summary data of experiments as illustrated in (**H**), demonstrating inhibition of calcein release by Gap27 but not by $Gap27^{Scr}$. Stars compare to control; number sign compares to BK. (**J**) Polymerase chain reaction demonstrating the absence of Panx1 mRNA in RBE4 and BCEC. C6-Panx1-Myc and C6-Panx-GFP are positive controls; RT− is a negative control; glyceraldehyde-3-phosphate dehydrogenase (GAPDH) is an internal control. The Western blot shown on the right demonstrates the absence of $P2X_7$ in RBE4; HEK-$P2X_7$ is a positive control. GFP, green fluorescent protein; RT, reverse transcriptase.

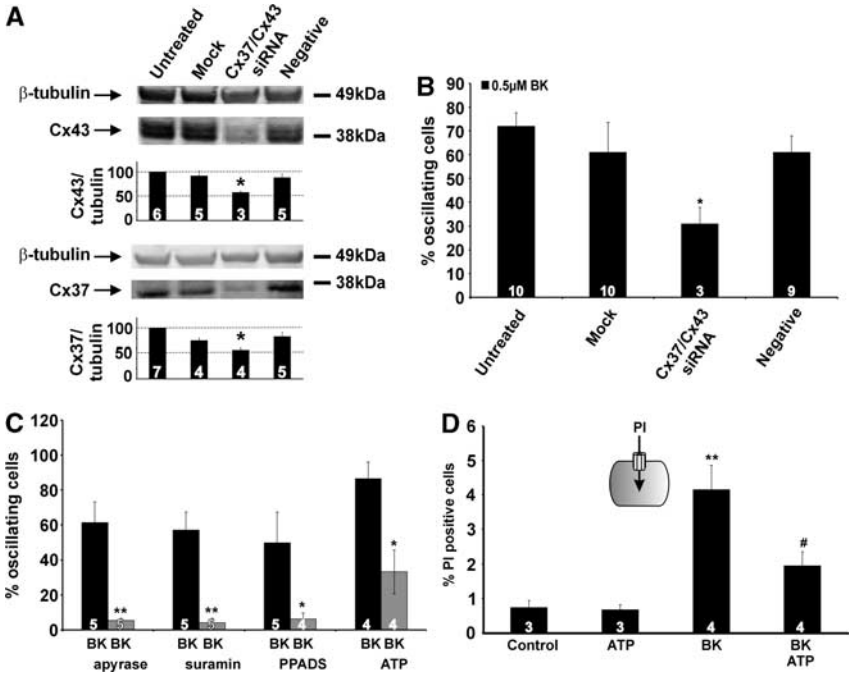

Figure 3 Effect of Cx37/43 gene silencing and contribution of purinergic signaling in bradykinin (BK)-triggered oscillations in the cytoplasmic Ca^{2+} concentration ($[Ca^{2+}]_i$). (**A**) siRNA suppression of Cx37 and Cx43 in rat brain endothelial (RBE4) cells, demonstrating significantly reduced expression to ~2/3 of the negative control signal (star symbol compares to negative control). (**B**) Cx37/Cx43 knockdown in RBE4 approximately halved the number of oscillating cells (star compares to negative control). (**C**) BK-triggered $[Ca^{2+}]_i$ oscillations were strongly reduced by apyrase VI/VII (5 U/mL, 30 minutes), suramin (200 μmol/L, 30 minutes) or pyridoxal phosphate-6-azo(benzene-2,4-disulfonic acid) tetrasodium salt (PPADS) (75 μmol/L, 30 minutes). Coexposure of BK together with adenosine 5′ triphosphate (ATP) (0.5 μmol/L) resulted in significantly reduced oscillatory activity. Stars compare to BK. (**D**) Propidium iodide (PI) dye uptake in RBE4 cells, demonstrating that BK (0.5 μmol/L) triggered an increase in the number of PI-positive cells whereas ATP (0.5 μmol/L) had no effect. Including ATP (0.5 μmol/L) together with BK inhibited the BK-triggered increase in dye uptake. Stars compare to control; number signs compare to BK.

transients/10 minutes; Figure 4B). The amplitudes of ATP-triggered oscillations (0.5 μmol/L) were smaller than those triggered by BK in RBE4 cells but they were equal in BCECs (cocultured with glial cells), the cell system in which *in vitro* permeability measurements were made (see below) (Figure 4C). As observed with BK, ATP-triggered oscillatory activity (0.5 μmol/L) was significantly suppressed when glial cells were absent during coculture (2.8% ± 2.4% oscillating cells compared with 63.0% ± 18.3% with glial cells present during coculture, $n = 7$). Importantly, hemichannel PI uptake studies in RBE4 cells demonstrated no hemichannel opening in response to ATP (Figure 3D) and ATP-induced oscillations were not influenced by Cbx and Gap27 (Figure 4D), indicating an oscillation mechanism that is distinct from BK-triggered oscillations.

Bradykinin, but not Adenosine 5′ Triphosphate, Increases Bovine Brain Capillary Endothelial Cell Permeability in a $[Ca^{2+}]_i$-Dependent and Gap27-Inhibitable Manner

We tested the effect of BK and ATP on the permeability of BCECs grown on filter membranes in the presence of glial cells (Cecchelli *et al*, 1999). Exposure to BK (0.5 μmol/L, present during the 60-minute duration of the permeability assay) increased the endothelial permeability measured with LY. Treatment with BK did not have any effect on BCEC cell death (0.5% ± 0.2% and 0.8% ± 0.3% PI-positive cells in untreated and BK-treated cultures, respectively, $n = 5$). Preloading of the BCECs with the Ca^{2+} buffer BAPTA (BAPTA-AM ester loading, 5 μmol/L, 1 hour), to restrain the induced $[Ca^{2+}]_i$ changes, or incubation of the cells with Gap27 (200 μmol/L, 30 minutes preincubation and present during the permeability assay) prevented the permeability increase brought about by BK (Figures 5B–5D). In contrast to BK, ATP (0.5 μmol/L) had no influence on endothelial permeability (Figure 5E), which is in line with the observations in other endothelia where ATP has no effect on permeability (Jacobson *et al*, 2006). Applying higher ATP concentrations (5 μmol/L) or the more potent P2Y receptor agonist 2-MeS-ATP (0.5 μmol/L), as well as combining ATP exposure with ARL-67156 (100 μmol/L) to inhibit ATP degradation by ecto-ATPases were all without effect on endothelial permeability (data not shown).

We further probed the BK-triggered permeability increase with 3 kDa DF instead of LY (457 Da) as a

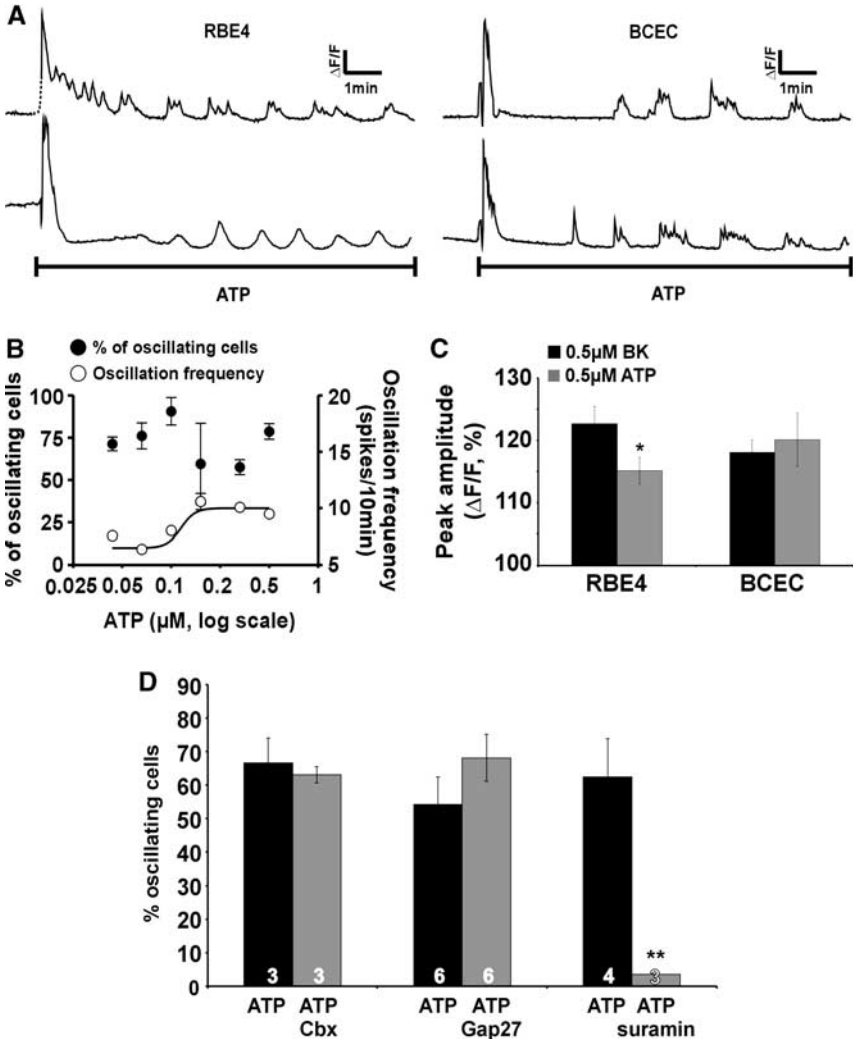

Figure 4 Adenosine 5′ triphosphate (ATP) elicits oscillations in the cytoplasmic Ca^{2+} concentration ($[Ca^{2+}]_i$) that are not influenced by connexin channel blockers. (**A**) Example traces demonstrating $[Ca^{2+}]_i$ oscillations triggered by 0.5 μmol/L ATP in selected rat brain endothelial (RBE4) and bovine brain capillary endothelial cells (BCECs). (**B**) Percentage of oscillating cells (●, left ordinate) and oscillation frequency (○, right ordinate) for various ATP concentrations. (**C**) Comparison of the peak amplitudes of $[Ca^{2+}]_i$ oscillations obtained with bradykinin (BK) and ATP. The amplitudes were slightly (but significantly) different in RBE4 but not different in BCECs, the cells used for endothelial permeability measurements presented in Figure 5. (**D**) ATP-induced $[Ca^{2+}]_i$ oscillations disappeared with suramin (200 μmol/L, 30 minutes) but were not influenced by Cbx (25 μmol/L, 30 minutes) and Gap27 (200 μmol/L, 1 hour). Stars compare to the neighboring black bar.

reporter dye, to obtain information on the permeability profile. The BK-triggered permeability increase (expressed as fold increase) was very similar when assessed with these two dyes, as illustrated in Table 1. Because the results of the experiments presented in Figure 3D suggest connexin hemichannel opening upon BK exposure, we tested the possibility that hemichannel opening at both sides of the endothelial plasma membrane creates a transcellular passageway for reporter dyes. We therefore applied LY and 3 kDa DF in hemichannel dye uptake experiments. These experiments showed that BK-triggered dye uptake in RBE4 cells was very different with the two probes, displaying no significant dye uptake of 3 kDa DF and an almost threefold increase (compared with control) when probed with LY (Table 1). These distinct permeation profiles for increased endothelial permeability versus hemichannel opening indicate that hemichannels do not contribute as a direct, transcellular pathway to increased endothelial permeability as measured with the 3 kDa DF probe.

In a next step, we investigated whether Gap27 was able to limit BBB permeability changes induced by BK *in vivo*. Bradykinin was injected intravenously (150 μg/kg) together with 3 kDa DF (30 mg/kg) as a marker for endothelial permeability. After 30 minutes, the animals were killed and coronal brain slices were cut. These experiments showed an enhanced fluorescence signal as quantified in the cortical regions, demonstrating increased leakage of reporter dye from the vascular lumen into the tissue. When

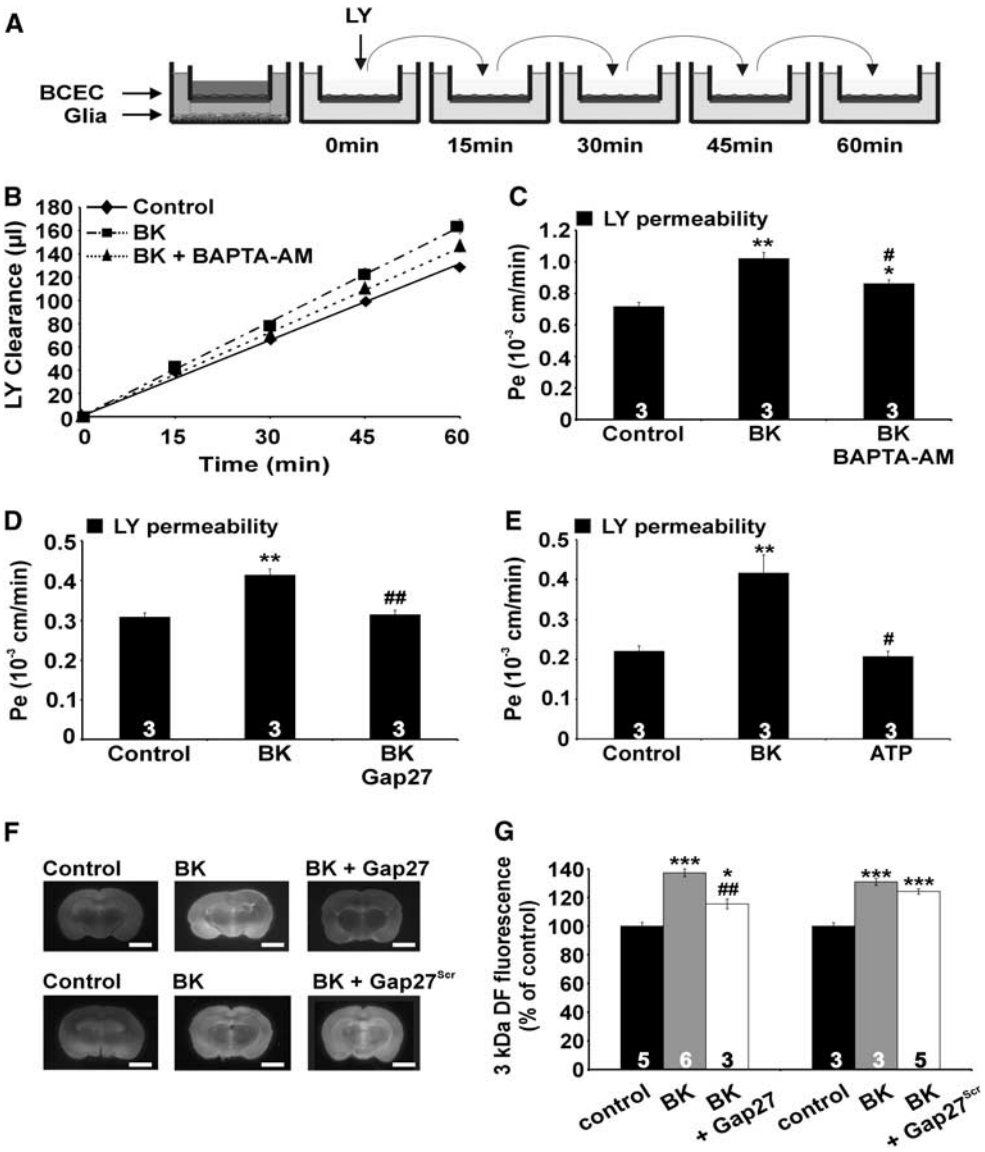

Figure 5 Effects of bradykinin (BK) and adenosine 5′ triphosphate (ATP) on endothelial permeability. (**A**) *In vitro* permeability measurements. Bovine brain capillary endothelial cells (BCECs) were grown on membrane inserts in noncontact coculture with glial cells at the bottom of the well. Membrane inserts were then placed in a new well and the fluorescent marker lucifer yellow (LY) was added. (**B**) Example curves for LY clearance from which the permeability coefficient Pe was calculated. BK (0.5 μmol/L) was added in the upper compartment; loading with 1,2-bis-(2-aminophenoxy)-ethane-*N,N,N′,N′*-tetraacetic acid acetoxy methyl ester (BAPTA-AM; 1 hour) was performed with 5 μmol/L in the upper compartment, in a well without glia. (**C**) Summary data of experiments as illustrated in (**B**). BK (0.5 μmol/L) significantly increased the permeability to LY and this effect was inhibited by preloading BCECs with BAPTA-AM. (**D**) The BK-triggered permeability increase was significantly reduced by Gap27 (200 μmol/L, 1 hour preincubation in upper and lower compartment without glia, and present during the permeability assay). (**E**) ATP (0.5 μmol/L, upper compartment) did not influence endothelial permeability, in contrast to BK. (**F**) *In vivo* blood–brain barrier (BBB) permeability measurements. Coronal brain sections demonstrating that BK (150 μg/kg, intravenously) increased the leakage of 3 kDa dextran fluorescein (DF) in the neural tissue determined 30 minutes after BK/3 kDa DF injection. Administration of BK/3 kDa DF together with Gap27 (25 mg/kg) decreased the tissue leakage of the fluorescent marker while Gap27^{Scr} had no effect. Scale bar represents 0.5 cm. (**G**) Summary data of experiments as illustrated in (**F**). The fluorescence intensity was measured in 10 analysis points in the cortical zones. Gap27 significantly reduced 3 kDa DF leakage, while Gap27^{Scr} had no effect. Stars compare to control; number signs compare to BK.

the same experiment was performed with Gap27 (25 mg/kg, corresponding to $\sim$200 μmol/L assuming the blood compartment as the distribution volume) coadministered together with BK/3 kDa DF, the cortical fluorescence signal was significantly suppressed (Figures 5F and 5G), replicating the observations in the *in vitro* BBB model. In rats treated with Gap27^{Scr} (25 mg/kg), the BK-triggered permeability increase was not different from rats treated with BK alone. Thus, in addition to inhibiting BK-triggered

$[Ca^{2+}]_i$ oscillations, Gap27 also inhibits the BK-triggered elevation of endothelial permeability *in vitro* and *in vivo*.

Effects of Bradykinin and Gap27 Treatment on Tight Junction and Cytoskeletal Proteins

In a last step, we verified in BCECs whether BK exposure was associated with alterations in the organization of tight junction and cytoskeletal proteins. We did not observe any modifications in immunocytochemical stainings of occludin or ZO-1 and in phalloidin-stained F-actin (Figure 6A) following exposure to BK (0.5 μmol/L, 1 hour). We did, however, observe changes in the organization of the intermediate filament vimentin, with thickening, clustering, and stretching of the fibers as compared with untreated control cells. These BK-triggered alterations were absent in cells exposed to BK + Gap27 (200 μmol/L, 1 hour) or to ATP (0.5 μmol/L, 1 hour) (Figure 6A).

Discussion

The present work demonstrates that BK induces endothelial $[Ca^{2+}]_i$ oscillations that are inhibited by interfering with connexin channel function, making use of Cbx, Gap27 peptide or Cx37/43 knockdown. Bradykinin triggered an increase of *in vitro*-measured endothelial permeability, which was dependent on endothelial $[Ca^{2+}]_i$ changes and was counteracted by inhibiting $[Ca^{2+}]_i$ oscillations with Gap27. Moreover, Gap27 also inhibited BK-triggered BBB permeability elevation *in vivo*. ATP-triggered oscillations were not influenced by interfering with connexin channels and ATP did not alter *in vitro*-measured endothelial permeability. The rapid effect of Gap27 on BK-triggered oscillations, its inhibition of hemichannel dye uptake/release before having any effect on gap junctions, and the BK stimulation of dye uptake/release all point to hemichannel involvement in the BK-triggered oscillations. Collectively, these data suggest that the connexin channel linkage of BK-triggered $[Ca^{2+}]_i$ oscillations, which is absent in ATP-triggered oscillations, has a role in influencing BBB permeability.

Table 1 Overview of BK-triggered changes in *in vitro*-measured BCEC permeability and hemichannel dye uptake in RBE4

	Endothelial permeability	*Hemichannel dye uptake*
LY	1.5 ± 0.6	2.8 ± 0.7
3 kDa DF	1.5 ± 0.2	0.5 ± 0.4

BCEC, bovine brain capillary endothelial cell; BK, bradykinin; DF, dextran fluorescein; LY, lucifer yellow; RBE4, rat brain endothelial cells.
Numbers report the fold increase of dye passage/uptake provoked by 0.5 μmol/L BK and expressed relative to control ($n = 3$ for all).

Thus, Gap27 can be used to disrupt connexin channel-linked oscillations, thereby preventing BBB permeability changes.

BK is a well-known permeability-increasing substance in brain endothelium (Abbott, 2000; Sarker *et al*, 2000). Binding to its corresponding receptors produces the second messenger $InsP_3$ that triggers Ca^{2+} release from the endoplasmic reticulum (Easton and Abbott, 2002). Several downstream signals and targets further contribute to the effects of BK on brain endothelial permeability, including free radical formation (Easton and Abbott, 2002; Sarker *et al*, 2000), activation of Ca^{2+}- or ATP-sensitive potassium channels (Ningaraj *et al*, 2003), activation of VEGF receptors (Thuringer *et al*, 2002), and alterations in junctional proteins (Easton and Abbott, 2002; Liu *et al*, 2008). $InsP_3$, endoplasmic reticulum-located $InsP_3$ receptors and subsequent Ca^{2+} release are the necessary and sufficient ingredients to generate $[Ca^{2+}]_i$ oscillations (Dupont *et al*, 2007). Brain endothelial cells have been reported to display $[Ca^{2+}]_i$ oscillations in response to various stimuli and conditions, including ATP (Haorah *et al*, 2007), hypoxia (Brown *et al*, 2004), subarachnoid hemorrhage (Scharbrodt *et al*, 2009), infection (Nikolskaia *et al*, 2006), and lymphocyte migration (Etienne-Manneville *et al*, 2000). However, at present, the role of $[Ca^{2+}]_i$ oscillations in brain endothelial function is not clear.

The inhibition of BK-triggered $[Ca^{2+}]_i$ oscillations by Cbx, Gap27, and Cx37/43 knockdown demonstrates that interfering with connexin channels affects the oscillatory activity. The data obtained from dye uptake/dye release experiments, Cx37/43 silencing and Gap27 peptide, all point to the involvement of unapposed connexin hemichannels. Gap27 is known to inhibit gap junctions but we show here that 1 hour exposure to the peptide has no effect on gap junctional coupling, in line with previous work in other cell types (Decrock *et al*, 2009; Evans *et al*, 2006). Instead, hemichannel dye uptake/release was strongly inhibited by the peptide and recent single-channel electrophysiological studies indicate that Gap27 inhibits unitary currents through Cx37 and Cx43 hemichannels with a time constant of 2 to 4 minutes (unpublished observation). This appears to be confirmed in the results depicted in Figure 2E, demonstrating rapid disappearance of oscillations upon addition of Gap27, and Figure 2H, illustrating fast-onset effects on the slope of calcein release. Side effects of Gap27 on other targets, like the $InsP_3$-Ca^{2+} signaling-axis that forms the basis of the $[Ca^{2+}]_i$ oscillation machinery (Dupont *et al*, 2007), were excluded based on $InsP_3$ photoliberation experiments in C6-glioma cells. A contribution of hemichannels composed of Panx1 was excluded based on the absence of Panx1 mRNA.

Connexin hemichannels form a release pathway for ATP (Kang *et al*, 2008) and purinergic signaling was involved in BK-triggered oscillations, as apyrase, suramin and PPADS all suppressed the oscillations.

The contribution of purinergic signaling in BK-triggered oscillations is likely to be autocrine because a paracrine contribution would be associated with time- or phase-related $[Ca^{2+}]_i$ changes in surrounding cells, which was not observed. Connexin hemichannels also form a pathway for Ca^{2+} entry into the cell

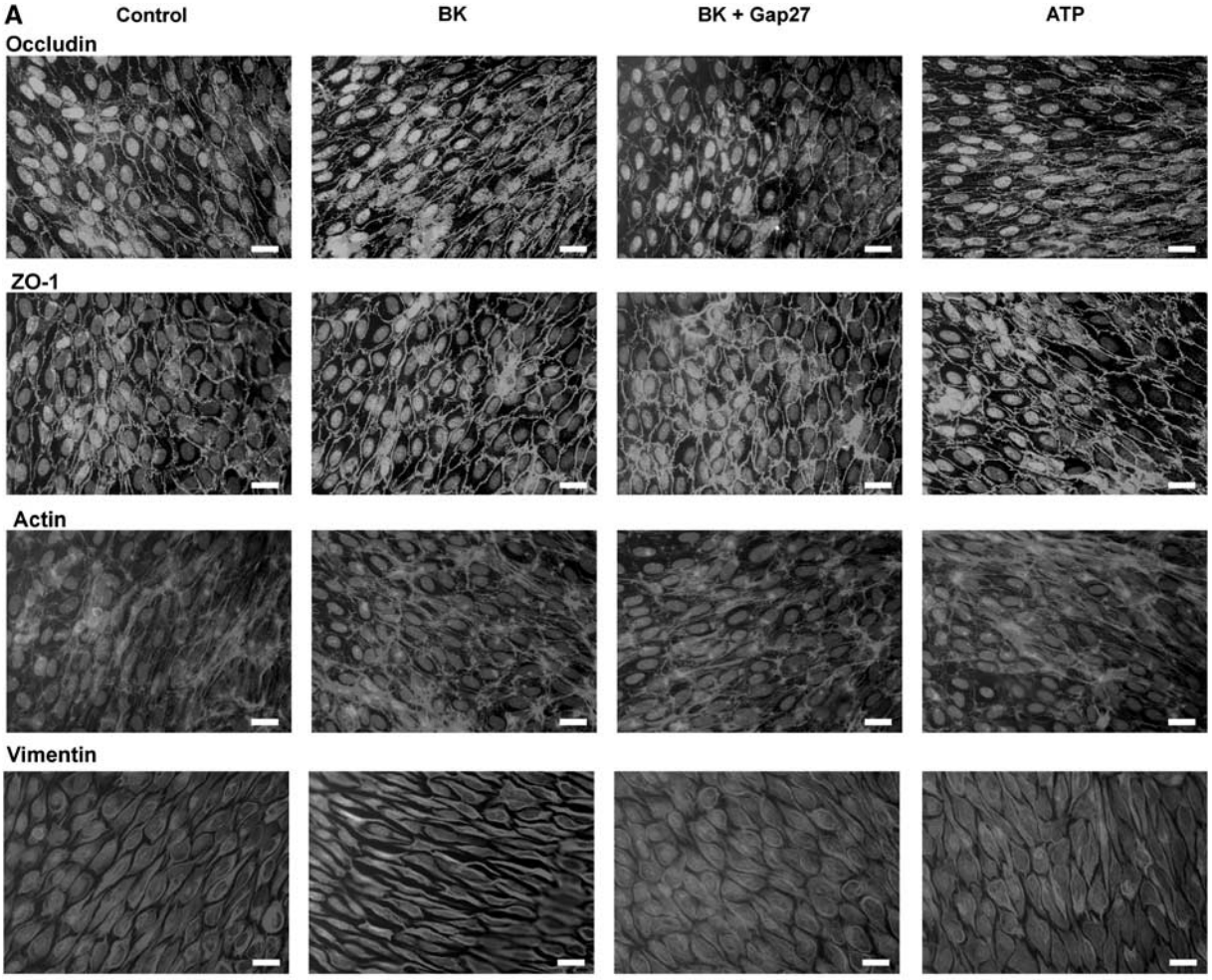

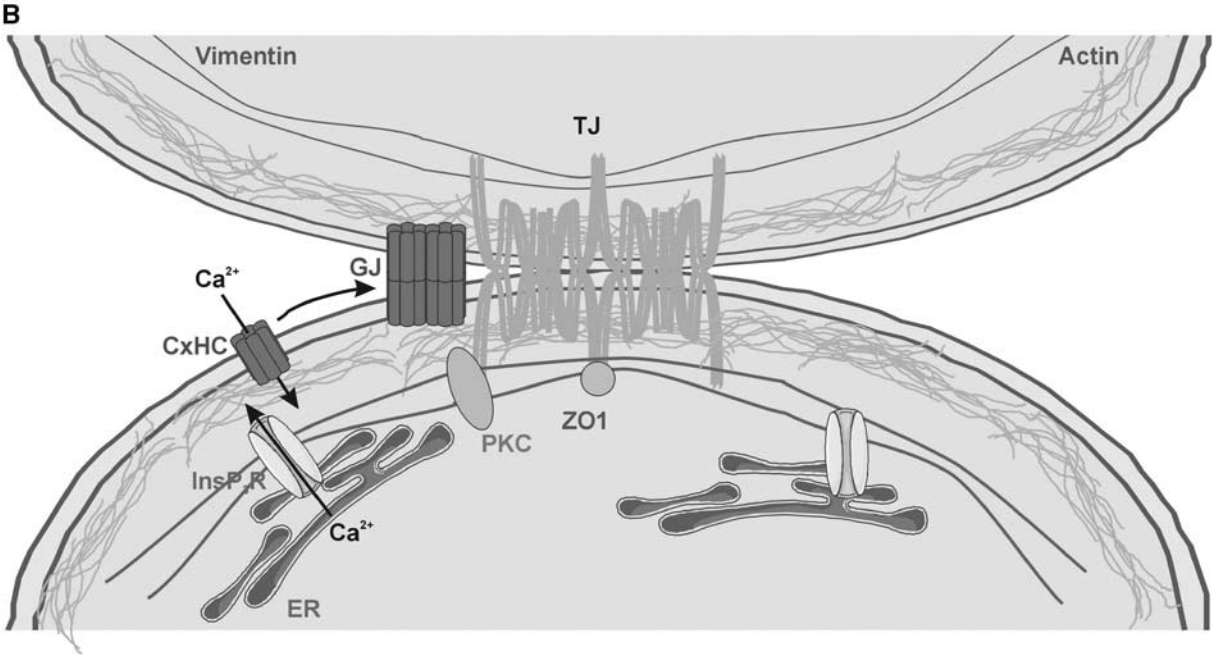

(Schalper *et al*, 2010; Verma *et al*, 2009), which is necessary for sustained $[Ca^{2+}]_i$ oscillations (Berridge, 2007). In addition to forming a Ca^{2+} entry pathway, connexin hemichannels are also activated by $[Ca^{2+}]_i$ changes (De Vuyst *et al*, 2006; Ponsaerts *et al*, 2010). Thus, hemichannels are expected to open with each oscillatory $[Ca^{2+}]_i$ spike, thereby opening a Ca^{2+} entry pathway. In addition, every $[Ca^{2+}]_i$ spike will be associated with ATP release via hemichannels, with subsequent autocrine activation of P2Y receptors (P_2Y_1 and P_2Y_2) (Albert *et al*, 1997) and increased generation of $InsP_3$. This will result in repetitive increases in $InsP_3$ concentration that are known to support $[Ca^{2+}]_i$ oscillations (Nash *et al*, 2001). Inhibiting connexin hemichannels with Gap27 may thus disrupt the BK-triggered oscillations by limiting Ca^{2+} entry and $InsP_3$ generation, two fundamental modulators of $[Ca^{2+}]_i$ oscillations. $[Ca^{2+}]_i$ oscillations triggered by ATP were, on the other hand, not influenced by Cbx and Gap27, which is in line with the observation that ATP did not trigger PI uptake and hemichannel opening. The BK-triggered oscillations thus involve hemichannel opening while those triggered by ATP do not activate this pathway. Moreover, the simultaneous activation of two distinct oscillation mechanisms by coapplying BK and ATP, stopped the $[Ca^{2+}]_i$ oscillations and prevented hemichannel opening, adding further evidence that hemichannel opening contributes to the oscillations.

Connexin proteins are transported via the endoplasmic reticulum and Golgi apparatus to the plasma membrane, where they appear as hexameric hemichannels. Plasma membrane hemichannels can diffuse laterally on their way to becoming incorporated into gap junction plaques (Laird, 2006), which are located at the nexus between endothelial cells, together with the tight junctional proteins (Lum *et al*, 1999). $InsP_3$ receptors and protein kinase C, which is a possible intermediate effector between $[Ca^{2+}]_i$ and endothelial permeability changes, are also situated at the nexus (Colosetti *et al*, 2003; Stamatovic *et al*, 2006) (Figure 6B). Taken together, we speculate that the hemichannel Ca^{2+} entry/purinergic signaling pathway activated by BK is located close to the nexus and may be well positioned to result in spatially restricted $[Ca^{2+}]_i$ changes at the very place where they are needed to influence the tight junction proteins and to alter the paracellular permeability. We found evidence for BK-induced changes at the level of vimentin fibers, without accompanying effects on occludin, ZO-1 or F-actin organization. These BK-triggered alterations were absent with Gap27 treatment and were not observed with ATP. At present, it is not clear how $[Ca^{2+}]_i$ changes would affect vimentin organization, but there is some evidence that $[Ca^{2+}]_i$ is involved in endothelin-1-induced vimentin reorganization (Chen *et al*, 2003) and that vimentin signaling has a role in *Escherichia coli* invasion of brain endothelial cells (Chi *et al*, 2010). In addition to affecting paracellular permeability, BK has also been reported to favor the transcellular route (Jungmann *et al*, 2008) by increasing endocytosis whereby the fusion of endocytotic vesicles may lead to the formation of 'transcellular channels' (Neal and Michel, 1995). An alternative formed by the opening of connexin hemichannels in the luminal and abluminal endothelial membranes is possible (Table 1) but is limited to below 1.5 kDa molecules as expected from the permeability properties of these channels (Kondo *et al*, 2000; Li *et al*, 1996). Finally, it needs to be stressed that BBB permeability *in vivo* is regulated not only by the endothelium in close cooperation with astrocytes (Boveri *et al*, 2005) but also by pericytes (Bell *et al*, 2010) and neurons, that is by the cells forming the neurovascular unit (Neuwelt *et al*, 2011; Zlokovic, 2008). At present, we do not know whether these cells have any influence on connexin channel functioning and/or endothelial $[Ca^{2+}]_i$ oscillations. The findings presented in this paper indicate that glial cells are necessary for BK- and ATP-triggered endothelial $[Ca^{2+}]_i$ oscillations.

In conclusion, this work shows that Gap27 inhibits BK-triggered $[Ca^{2+}]_i$ oscillations and endothelial permeability changes, thereby bringing up a novel connexin-related pathway that may be exploited to limit BBB permeability increases under pathological conditions like brain ischemia and trauma. In contrast to inhibiting gap junctions, which results in a loss of barrier function (Nagasawa *et al*, 2006), inhibition of hemichannels appears to preserve barrier function.

Figure 6 Alterations at the level of tight junctions and cytoskeletal proteins, and summary scheme. (**A**) Representative images of occludin, ZO-1, F-actin, and vimentin staining in bovine brain capillary endothelial cell (BCEC) under the various experimental conditions indicated. Vimentin filaments appeared more condense and stretched after bradykinin (BK) exposure (0.5 μmol/L, 1 hour), and this was not observed with BK + Gap27 (200 μmol/L, 1 hour) or adenosine 5′ triphosphate (ATP) (0.5 μmol/L, 1 hour). The data shown are representative for four different experiments (scale bar is 25 μm). (**B**) Summary scheme sketching a possible scenario for hemichannel involvement in BK-triggered blood–brain barrier (BBB) permeability increases. Endothelial junctions are zipper-like structures containing tight junctions (TJ) and gap junctions (GJ). Connexin hemichannels (CxHC) are transported to the plasma membrane and diffuse laterally (arrow) to become incorporated into gap junctions. Tight junctions, cytoskeletal proteins, $InsP_3$ receptors, PKC, gap junctions, and hemichannels are all in close association at the nexus. $InsP_3$ receptors ($InsP_3R$) form the basis of Ca^{2+} concentration ($[Ca^{2+}]_i$) oscillations. BK-triggered oscillations are associated with hemichannel opening while those triggered by ATP do not activate the hemichannel pathway (for unknown reasons). Hemichannel opening results in Ca^{2+} entry thereby affecting tight junction/cytoskeletal proteins directly or via intermediate signaling steps involving PKC. PKC, protein kinase C.

Acknowledgements

This work could not have been successfully completed without the help of K Leurs, C Mabilde, E Tack, and everyone at the LBHE (Laboratoire de Physiopathologie de la Barrière Hémato-Encéphalique).

Disclosure/conflict of interest

The authors declare no conflict of interest.

References

Abbott NJ (2000) Inflammatory mediators and modulation of blood-brain barrier permeability. *Cell Mol Neurobiol* 20:131–47

Albert JL, Boyle JP, Roberts JA, Challiss RA, Gubby SE, Boarder MR (1997) Regulation of brain capillary endothelial cells by P2Y receptors coupled to Ca2+, phospholipase C and mitogen-activated protein kinase. *Br J Pharmacol* 122:935–41

Austinat M, Braeuninger S, Pesquero JB, Brede M, Bader M, Stoll G, Renne T, Kleinschnitz C (2009) Blockade of bradykinin receptor B1 but not bradykinin receptor B2 provides protection from cerebral infarction and brain edema. *Stroke* 40:285–93

Bell RD, Winkler EA, Sagare AP, Singh I, LaRue B, Deane R, Zlokovic BV (2010) Pericytes control key neurovascular functions and neuronal phenotype in the adult brain and during brain aging. *Neuron* 68:409–27

Berridge MJ (2007) Inositol trisphosphate and calcium oscillations. *Biochem Soc Symp* 74:1–7

Boveri M, Berezowski V, Price A, Slupek S, Lenfant AM, Benaud C, Hartung T, Cecchelli R, Prieto P, Dehouck MP (2005) Induction of blood-brain barrier properties in cultured brain capillary endothelial cells: comparison between primary glial cells and C6 cell line. *Glia* 51:187–98

Braet K, Aspeslagh S, Vandamme W, Willecke K, Martin PE, Evans WH, Leybaert L (2003) Pharmacological sensitivity of ATP release triggered by photoliberation of inositol-1,4,5-trisphosphate and zero extracellular calcium in brain endothelial cells. *J Cell Physiol* 197:205–13

Brown RC, Mark KS, Egleton RD, Davis TP (2004) Protection against hypoxia-induced blood-brain barrier disruption: changes in intracellular calcium. *Am J Physiol Cell Physiol* 286:C1045–52

Carter TD, Bogle RG, Bjaaland T (1991) Spiking of intracellular calcium ion concentration in single cultured pig aortic endothelial cells stimulated with ATP or bradykinin. *Biochem J* 278(Part 3):697–704

Cecchelli R, Dehouck B, Descamps L, Fenart L, Buee-Scherrer VV, Duhem C, Lundquist S, Rentfel M, Torpier G, Dehouck MP (1999) *In vitro* model for evaluating drug transport across the blood-brain barrier. *Adv Drug Deliv Rev* 36:165–78

Chen Y, McCarron RM, Golech S, Bembry J, Ford B, Lenz FA, Azzam N, Spatz M (2003) ET-1- and NO-mediated signal transduction pathway in human brain capillary endothelial cells. *Am J Physiol Cell Physiol* 284:C243–9

Chi F, Jong TD, Wang L, Ouyang Y, Wu C, Li W, Huang SH (2010) Vimentin-mediated signalling is required for IbeA+ E. coli K1 invasion of human brain microvascular endothelial cells. *Biochem J* 427:79–90

Colosetti P, Tunwell RE, Cruttwell C, Arsanto JP, Mauger JP, Cassio D (2003) The type 3 inositol 1,4,5-trisphosphate receptor is concentrated at the tight junction level in polarized MDCK cells. *J Cell Sci* 116:2791–803

De Blasio BF, Rottingen JA, Sand KL, Giaever I, Iversen JG (2004) Global, synchronous oscillations in cytosolic calcium and adherence in bradykinin-stimulated Madin-Darby canine kidney cells. *Acta Physiol Scand* 180:335–46

De Vuyst E, Decrock E, Cabooter L, Dubyak GR, Naus CC, Evans WH, Leybaert L (2006) Intracellular calcium changes trigger connexin 32 hemichannel opening. *EMBO J* 25:34–44

Decrock E, De Vuyst E, Vinken M, Van Moorhem M, Vranckx K, Wang N, Van Laeken L, De Bock M, D'Herde K, Lai CP, Rogiers V, Evans WH, Naus CC, Leybaert L (2009) Connexin 43 hemichannels contribute to the propagation of apoptotic cell death in a rat C6 glioma cell model. *Cell Death Differ* 16:151–63

Descamps L, Coisne C, Dehouck B, Cecchelli R, Torpier G (2003) Protective effect of glial cells against lipopolysaccharide-mediated blood-brain barrier injury. *Glia* 42:46–58

Doctrow SR, Abelleira SM, Curry LA, Heller-Harrison R, Kozarich JW, Malfroy B, McCarroll LA, Morgan KG, Morrow AR, Musso GF (1994) The bradykinin analog RMP-7 increases intracellular free calcium levels in rat brain microvascular endothelial cells. *J Pharmacol Exp Ther* 271:229–37

Dupont G, Combettes L, Leybaert L (2007) Calcium dynamics: spatio-temporal organization from the subcellular to the organ level. *Int Rev Cytol* 261:193–245

Easton AS, Abbott NJ (2002) Bradykinin increases permeability by calcium and 5-lipoxygenase in the ECV304/C6 cell culture model of the blood-brain barrier. *Brain Res* 953:157–69

Eltzschig HK, Eckle T, Mager A, Kuper N, Karcher C, Weissmuller T, Boengler K, Schulz R, Robson SC, Colgan SP (2006) ATP release from activated neutrophils occurs via connexin 43 and modulates adenosine-dependent endothelial cell function. *Circ Res* 99:1100–8

Etienne-Manneville S, Manneville JB, Adamson P, Wilbourn B, Greenwood J, Couraud PO (2000) ICAM-1-coupled cytoskeletal rearrangements and transendothelial lymphocyte migration involve intracellular calcium signaling in brain endothelial cell lines. *J Immunol* 165:3375–83

Evans WH, De Vuyst E, Leybaert L (2006) The gap junction cellular internet: connexin hemichannels enter the signalling limelight. *Biochem J* 397:1–14

Giaume C, Theis M (2010) Pharmacological and genetic approaches to study connexin-mediated channels in glial cells of the central nervous system. *Brain Res Rev* 63:160–76

Haorah J, Knipe B, Gorantla S, Zheng J, Persidsky Y (2007) Alcohol-induced blood-brain barrier dysfunction is mediated via inositol 1,4,5-triphosphate receptor (IP3R)-gated intracellular calcium release. *J Neurochem* 100:324–36

Hurst RD, Clark JB (1998) Alterations in transendothelial electrical resistance by vasoactive agonists and cyclic AMP in a blood-brain barrier model system. *Neurochem Res* 23:149–54

Jacobson JR, Dudek SM, Singleton PA, Kolosova IA, Verin AD, Garcia JG (2006) Endothelial cell barrier enhancement by ATP is mediated by the small GTPase Rac and cortactin. *Am J Physiol Lung Cell Mol Physiol* 291:L289–95

Jungmann P, Wilhelmi M, Oberleithner H, Riethmuller C (2008) Bradykinin does not induce gap formation between human endothelial cells. *Pflugers Arch* 455:1007–16

Kang J, Kang N, Lovatt D, Torres A, Zhao Z, Lin J, Nedergaard M (2008) Connexin 43 hemichannels are permeable to ATP. *J Neurosci* 28:4702–11

Kawano S, Otsu K, Kuruma A, Shoji S, Yanagida E, Muto Y, Yoshikawa F, Hirayama Y, Mikoshiba K, Furuichi T (2006) ATP autocrine/paracrine signaling induces calcium oscillations and NFAT activation in human mesenchymal stem cells. *Cell Calcium* 39:313–24

Kondo RP, Wang SY, John SA, Weiss JN, Goldhaber JI (2000) Metabolic inhibition activates a non-selective current through connexin hemichannels in isolated ventricular myocytes. *J Mol Cell Cardiol* 32:1859–72

Laird DW (2006) Life cycle of connexins in health and disease. *Biochem J* 394:527–43

Laskey RE, Adams DJ, Cannell M, van Breemen C (1992) Calcium entry-dependent oscillations of cytoplasmic calcium concentration in cultured endothelial cell monolayers. *Proc Natl Acad Sci USA* 89:1690–4

Li H, Liu TF, Lazrak A, Peracchia C, Goldberg GS, Lampe PD, Johnson RG (1996) Properties and regulation of gap junctional hemichannels in the plasma membranes of cultured cells. *J Cell Biol* 134:1019–30

Liu LB, Xue YX, Liu YH, Wang YB (2008) Bradykinin increases blood-tumor barrier permeability by down-regulating the expression levels of ZO-1, occludin, and claudin-5 and rearranging actin cytoskeleton. *J Neurosci Res* 86:1153–68

Lum H, Jaffe HA, Schulz IT, Masood A, RayChaudhury A, Green RD (1999) Expression of PKA inhibitor (PKI) gene abolishes cAMP-mediated protection to endothelial barrier dysfunction. *Am J Physiol* 277:C580–8

Nagasawa K, Chiba H, Fujita H, Kojima T, Saito T, Endo T, Sawada N (2006) Possible involvement of gap junctions in the barrier function of tight junctions of brain and lung endothelial cells. *J Cell Physiol* 208:123–32

Nash MS, Young KW, Challiss RA, Nahorski SR (2001) Intracellular signalling. Receptor-specific messenger oscillations. *Nature* 413:381–2

Neal CR, Michel CC (1995) Transcellular gaps in microvascular walls of frog and rat when permeability is increased by perfusion with the ionophore A23187. *J Physiol* 488(Part 2):427–37

Neuwelt EA, Bauer B, Fahlke C, Fricker G, Iadecola C, Janigro D, Leybaert L, Molnar Z, O'Donnell ME, Povlishock JT, Saunders NR, Sharp F, Stanimirovic D, Watts RJ, Drewes LR (2011) Engaging neuroscience to advance translational research in brain barrier biology. *Nat Rev Neurosci* 12:169–82

Nikolskaia OV, de ALAP, Kim YV, Lonsdale-Eccles JD, Fukuma T, Scharfstein J, Grab DJ (2006) Blood-brain barrier traversal by African trypanosomes requires calcium signaling induced by parasite cysteine protease. *J Clin Invest* 116:2739–47

Ningaraj NS, Rao MK, Black KL (2003) Adenosine 5′-triphosphate-sensitive potassium channel-mediated blood-brain tumor barrier permeability increase in a rat brain tumor model. *Cancer Res* 63:8899–911

Olesen SP (1989) An electrophysiological study of microvascular permeability and its modulation by chemical mediators. *Acta Physiol Scand Suppl* 579:1–28

Ponsaerts R, De Vuyst E, Retamal M, D'Hondt C, Vermeire D, Wang N, De Smedt H, Zimmermann P, Himpens B, Vereecke J, Leybaert L, Bultynck G (2010) Intramolecular loop/tail interactions are essential for connexin 43-hemichannel activity. *FASEB J* 24:4378–95

Raslan F, Schwarz T, Meuth SG, Austinat M, Bader M, Renne T, Roosen K, Stoll G, Siren AL, Kleinschnitz C (2010) Inhibition of bradykinin receptor B1 protects mice from focal brain injury by reducing blood-brain barrier leakage and inflammation. *J Cereb Blood Flow Metab* 30:1477–86

Sage SO, Adams DJ, van Breemen C (1989) Synchronized oscillations in cytoplasmic free calcium concentration in confluent bradykinin-stimulated bovine pulmonary artery endothelial cell monolayers. *J Biol Chem* 264:6–9

Sarker MH, Hu DE, Fraser PA (2000) Acute effects of bradykinin on cerebral microvascular permeability in the anaesthetized rat. *J Physiol* 528(Part 1):177–87

Schalper KA, Sanchez HA, Lee SC, Altenberg GA, Nathanson MH, Saez JC (2010) Connexin43 hemichannels mediate the Ca2+ influx induced by extracellular alkalinization. *Am J Physiol Cell Physiol* 299: C1504–15

Scharbrodt W, Abdallah Y, Kasseckert SA, Gligorievski D, Piper HM, Boker DK, Deinsberger W, Oertel MF (2009) Cytosolic Ca2+ oscillations in human cerebrovascular endothelial cells after subarachnoid hemorrhage. *J Cereb Blood Flow Metab* 29:57–65

Simon AM, Chen H, Jackson CL (2006) Cx37 and Cx43 localize to zona pellucida in mouse ovarian follicles. *Cell Commun Adhes* 13:61–77

Stamatovic SM, Dimitrijevic OB, Keep RF, Andjelkovic AV (2006) Protein kinase Calpha-RhoA cross-talk in CCL2-induced alterations in brain endothelial permeability. *J Biol Chem* 281:8379–88

Thuringer D, Maulon L, Frelin C (2002) Rapid transactivation of the vascular endothelial growth factor receptor KDR/Flk-1 by the bradykinin B2 receptor contributes to endothelial nitric-oxide synthase activation in cardiac capillary endothelial cells. *J Biol Chem* 277:2028–32

Verma V, Hallett MB, Leybaert L, Martin PE, Evans WH (2009) Perturbing plasma membrane hemichannels attenuates calcium signalling in cardiac cells and HeLa cells expressing connexins. *Eur J Cell Biol* 88:79–90

Zlokovic BV (2008) The blood-brain barrier in health and chronic neurodegenerative disorders. *Neuron* 57:178–201